PHYSICS

Universal relations for ultracold reactive molecules

Mingyuan He^{1,2,3}*, Chenwei Lv¹*, Hai-Qing Lin⁴, Qi Zhou^{1,5†}

The realization of ultracold polar molecules in laboratories has pushed physics and chemistry to new realms. In particular, these polar molecules offer scientists unprecedented opportunities to explore chemical reactions in the ultracold regime where quantum effects become profound. However, a key question about how two-body losses depend on quantum correlations in interacting many-body systems remains open so far. Here, we present a number of universal relations that directly connect two-body losses to other physical observables, including the momentum distribution and density correlation functions. These relations, which are valid for arbitrary microscopic parameters, such as the particle number, the temperature, and the interaction strength, unfold the critical role of contacts, a fundamental quantity of dilute quantum systems, in determining the reaction rate of quantum reactive molecules in a many-body environment. Our work opens the door to an unexplored area intertwining quantum chemistry; atomic, molecular, and optical physics; and condensed matter physics.

Copyright © 2020
The Authors, some rights reserved; exclusive licensee
American Association for the Advancement of Science. No claim to original U.S. Government Works. Distributed under a Creative
Commons Attribution
NonCommercial
License 4.0 (CC BY-NC).

INTRODUCTION

In a temperature regime down to a few tens of nanokelvin, highly controllable polar molecules provide scientists with a powerful apparatus to study a vast range of new quantum phenomena in condensed matter physics, quantum information processing, and quantum chemistry (1-14), such as exotic quantum phases (15-18), quantum gates with fast switching times (19, 20), and quantum chemical reactions (9-13). In all these studies, the two-body loss is an essential ingredient leading to non-Hermitian phenomena. Similar to other chemical reactions, collisions between molecules may yield certain products and release energies, which allow particles to escape the traps. For instance, a prototypical reaction, KRb + KRb \rightarrow K₂ + Rb₂, is the major source causing the loss of KRb molecules. Undetectable complexes may also form, resulting in losses in the system of interest (10, 11).

Whereas chemical reactions are known for their complexities, taking into account quantum effects imposes an even bigger challenge to both physicists and chemists. The exponentially large degrees of freedom and quantum correlations built upon interactions make it difficult to quantitatively analyze the reactions. A standard approach is to consider two interacting particles, the reaction rate of which is trackable (21, 22). Although these results are applicable in many-body systems when the temperature is high enough and correlations between different pairs of particles are negligible, with decreasing the temperature, many-body correlations become profound and this approach fails. In particular, in the first realization of a degenerate Fermi gas of polar molecules, unusual behaviors of twobody losses were observed (12). In the absence of electric fields, the dipole moment vanishes and these polar molecules interact with van der Waals interactions. With decreasing the temperature, the suppression of the loss rate no longer agrees with the Bethe-Wigner threshold. Experimental results also indicated that the temperature dependence of the density fluctuation is similar to that of the loss

In this work, we show that universality exists in chemical reactions of ultracold reactive molecules. We implement contacts, the central quantity in dilute quantum systems (23–25), to establish universal relations between the two-body loss rate and other quantities including the momentum distribution and the density correlation function. Previously, two-body losses of zero-range potentials hosting inelastic s-wave scatterings were correlated to the s-wave contact (26, 27). In reality, chemical reactions happen in a finite range. Many systems are also characterized by high-partial-wave scatterings. For instance, single-component fermionic KRb molecules interact with p-wave scatterings (1, 12). It is thus required to formulate a theory applicable to generic short-range reactive interactions. To concretize discussions, we focus on single-component fermionic molecules. All our results can be straightforwardly generalized to other systems with arbitrary short-range interactions.

RESULTS

Loss rate and contacts

The Hamiltonian of *N* reactive molecules is written as

$$H = \sum_{i} \left[-\frac{\hbar^{2}}{2M} \nabla_{i}^{2} + V_{\text{ext}}(\mathbf{r}_{i}) \right] + \sum_{i>j} U(\mathbf{r}_{i} - \mathbf{r}_{j})$$
 (1)

where M is the molecular mass, $V_{\text{ext}}(\mathbf{r})$ is the external potential, and $U(\mathbf{r})$ is a two-body interaction, as shown in Fig. 1. The many-body wave function, $\Psi(\mathbf{r}_1, \mathbf{r}_2, ..., \mathbf{r}_N)$, satisfies the time-dependent Schrödinger equation

$$i\hbar \partial_t \Psi(\mathbf{r}_1, \mathbf{r}_2, ..., \mathbf{r}_N) = H\Psi(\mathbf{r}_1, \mathbf{r}_2, ..., \mathbf{r}_N)$$
 (2)

In the absence of electric fields, $U(\mathbf{r})$ is a short-range interaction with a characteristic length scale, r_0 . When $|\mathbf{r}| > r_0$, $U(\mathbf{r}) = 0$. Chemical reactions happen in an even shorter length scale, $r^* < r_0$. We adopt the one-channel model using a complex $U(\mathbf{r}) = U_R(\mathbf{r}) + iU_I(\mathbf{r})$ to describe the chemical reaction (22), where $U_I(\mathbf{r}) \le 0$. When $|\mathbf{r}| > r^*$, $U_I(\mathbf{r}) = 0$. Using the Lindblad equation that models the losses by jump operators, the same universal relations can also be derived (Materials and Methods).

rate (12, 14). A theory fully incorporating quantum many-body effects is, therefore, desired to understand the chemical reaction rate at low temperatures.

¹Department of Physics and Astronomy, Purdue University, West Lafayette, IN 47907, USA. ²Shenzhen JL Computational Science and Applied Research Institute, Shenzhen 518109, China. ³Department of Physics, Hong Kong University of Science and Technology, Clear Water Bay, Hong Kong, China. ⁴Beijing Computational Science Research Center, Beijing 100193, China. ⁵Purdue Quantum Science and Engineering Institute, Purdue University, West Lafayette, IN 47907, USA.

^{*}These authors contributed equally to this work.

[†]Corresponding author. Email: zhou753@purdue.edu

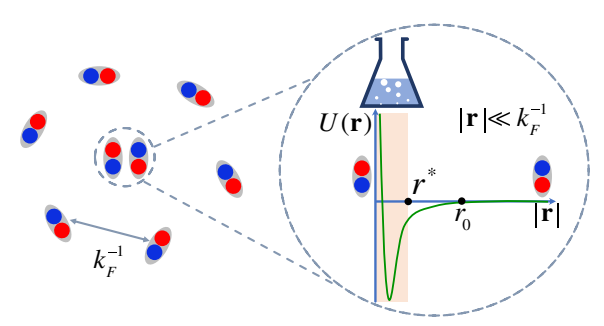


Fig. 1. A length scale separation in dilute molecules. The blue (red) solid spheres represent potassium (rubidium) atoms. Inside the dashed circle are two molecules, the separation between which is much smaller than the average interparticle spacing, $|\mathbf{r}| \ll k_F^{-1}$. The enlarged plot of the regime inside the dashed circle is a schematic of the chemical reaction. The green solid curve represents the real part of the interaction, $U_R(\mathbf{r})$. The imaginary part of the interaction, $U_I(\mathbf{r})$, is nonzero only in the shaded area, where the reaction happens.

Universal relations arise from a length scale separation in dilute quantum systems, $r^* < r_0 \ll k_F^{-1}$, where k_F^{-1} , the inverse of the Fermi momentum, captures the average interparticle separation. When the distance between two molecules is much smaller than k_F^{-1} , we obtain

$$\Psi(\mathbf{r}_{1},\mathbf{r}_{2},...,\mathbf{r}_{N}) \xrightarrow{|\mathbf{r}_{ij}| \ll k_{F}^{-1}} \sum_{m,\epsilon} \psi_{m}(\mathbf{r}_{ij};\epsilon) G_{m}(\mathbf{R}_{ij};E-\epsilon) \quad (3)$$

where $\mathbf{r}_{ij} = \mathbf{r}_i - \mathbf{r}_j$ denotes the relative coordinates of the ith and the jth molecules and $\mathbf{R}_{ij} = \{(\mathbf{r}_i + \mathbf{r}_j)/2, \mathbf{r}_{k \neq i,j}\}$ is a short-hand notation including coordinates of their center of mass and all other particles. $\psi_m(\mathbf{r}_{ij}; \boldsymbol{\epsilon})$ is a p-wave wave function with a magnetic quantum number $m = 0, \pm 1$, which is determined solely by the two-body Hamiltonian, $H_2 = -(\hbar^2/M)\nabla^2 + U(\mathbf{r}_{ij})$, as all other particles are far away from the chosen pair in the regime, $|\mathbf{r}_{ij}| \ll k_F^{-1}$. $G_m(\mathbf{R}_{ij}; E - \boldsymbol{\epsilon})$ includes all many-body effects, which depend on the center of mass of the ith and the jth molecules and all other N-2 molecules, and can be viewed as a "normalization factor" of the two-body wave function $\psi_m(\mathbf{r}_{ij}; \boldsymbol{\epsilon})$. E is the total energy of the many-body system. $\boldsymbol{\epsilon}$, the colliding energy, is no longer a good quantum number in a many-body system, and a sum shows up in Eq. 3. Since both a continuous spectrum and discrete bound states may exist, we use the notation of sum other than an integral.

Although $\psi_m(\mathbf{r}_{ij}; \boldsymbol{\epsilon})$ depends on the details of $U(\mathbf{r}_{ij})$ when $|\mathbf{r}_{ij}| < r_0$, it is universal when $r_0 < |\mathbf{r}_{ij}| \ll k_F^{-1}$, as a result of vanishing interaction in this regime. We define $\psi_m(\mathbf{r}_{ij}; \boldsymbol{\epsilon}) = \phi_m(|\mathbf{r}_{ij}|; \boldsymbol{\epsilon}) \, Y_{1m}(\hat{\mathbf{r}}_{ij})$, where $Y_{1m}(\hat{\mathbf{r}}_{ij})$ is the p-wave spherical harmonics. Whereas many resonances exist, the phase shift of the scattering between KRb molecules is still a smooth function of the energy, due to the large average line width of these resonances, which far exceeds the mean level spacing of the bound states (21). The phase shift, η , then has a well-defined expansion, $q_{\epsilon}^3 \cot \left[\eta \left(q_{\epsilon} \right) \right] = -1/v_p + q_{\epsilon}^2/r_e$, where v_p and r_e are the p-wave scattering volume and effective range, respectively, both of which are complex for reactive interactions. $q_{\epsilon} = (\epsilon M/\hbar^2)^{1/2}$. Consequently, $\phi_m(|\mathbf{r}_{ij}|; \boldsymbol{\epsilon}) = \phi_m^{(0)}(|\mathbf{r}_{ij}|) + q_{\epsilon}^2 \phi_m^{(1)}(|\mathbf{r}_{ij}|) + O(q_{\epsilon}^4)$, where

$$\varphi_m^{(0)}(|\mathbf{r}_{ij}|) \xrightarrow{r_0 < |\mathbf{r}_{ij}| \ll k_F^{-1}} \frac{1}{|\mathbf{r}_{ij}|^2} - \frac{1}{v_p} \frac{|\mathbf{r}_{ij}|}{3}$$
(4)

$$\varphi_m^{(1)}(|\mathbf{r}_{ij}|) \xrightarrow{r_0 < |\mathbf{r}_{ij}| \ll k_F^{-1}} \xrightarrow{1} \frac{|\mathbf{r}_{ij}|}{3} + \frac{1}{\nu_p} \frac{|\mathbf{r}_{ij}|^3}{30} + \frac{1}{2}$$
 (5)

To simplify expressions, we have considered isotropic p-wave interactions, $\varphi(|\mathbf{r}_{ij}|) = \varphi_m(|\mathbf{r}_{ij}|)$ and $G(\mathbf{R}_{ij}; E - \epsilon) = G_m(\mathbf{R}_{ij}; E - \epsilon)$, and suppressed other partial waves in the expressions, which do not show up in universal relations relevant for single-component fermionic molecules.

Using Eqs. 1 to 3, we find that the decay of the total particle number is captured by

$$\partial_t N = -\frac{\hbar}{8\pi^2 M} \sum_{\nu=1}^3 \kappa_\nu C_\nu \tag{6}$$

where the three contacts are written as

$$C_1 = 3 (4\pi)^2 N(N-1) \int d\mathbf{R}_{ij} |g^{(0)}|^2$$
 (7)

$$C_2 = 6 (4\pi)^2 N(N-1) \int d\mathbf{R}_{ij} \operatorname{Re}(g^{(0)*}g^{(1)})$$
 (8)

$$C_3 = 6 (4\pi)^2 N(N-1) \int d\mathbf{R}_{ij} \operatorname{Im}(g^{(0)*} g^{(1)})$$
 (9)

 $\int d\mathbf{R}_{ij} = \int d[(\mathbf{r}_i + \mathbf{r}_j)/2] d\mathbf{r}_{k \neq i,j}$ and $g^{(s)} = \sum_{\epsilon} q_{\epsilon}^{2s} G(\mathbf{R}_{ij}, E - \epsilon)$. As shown later, C_1 determines the leading term in the large momentum tail, similar to systems without losses (28–31). In contrast, $C_{2,3}$ are new quantities in systems with two-body losses.

 κ_{ν} in Eq. 6 are microscopic parameters determined purely by the two-body physics. In our one-channel model, their explicit expressions are given by

$$\kappa_1 = -\frac{M}{\hbar^2} \int_0^\infty U_I(r) \left| \phi^{(0)}(r) \right|^2 r^2 dr \tag{10}$$

$$\kappa_2 = -\frac{M}{\hbar^2} \text{Re} \left(\int_0^\infty U_I(r) \, \phi^{(0)*}(r) \, \phi^{(1)}(r) \, r^2 \, dr \right) \tag{11}$$

$$\kappa_3 = \frac{M}{\hbar^2} \text{Im} \left(\int_0^\infty U_I(r) \, \phi^{(0)*}(r) \, \phi^{(1)}(r) \, r^2 \, dr \right) \tag{12}$$

where $r=|\mathbf{r}|$. If $U(\mathbf{r})$ is modeled by two square well potentials, one for its real part and the other for its imaginary part, then $\kappa_{1,2,3}$ can be evaluated explicitly. For simplicity, we set $U(\mathbf{r})=-\tilde{U}_R-i\tilde{U}_I$ when $|\mathbf{r}|\leq r_0=r^*$ and 0 elsewhere. Changing the ratio r_0/r^* does not change any results qualitatively. Figure 2 shows how $\kappa_{1,2,3}$ depend on \tilde{U}_I when \tilde{U}_R is fixed at various values including those corresponding to small and divergent v_p in the absence of \tilde{U}_I . When $\tilde{U}_I=0$, $\kappa_{1,2,3}=0$. With increasing \tilde{U}_I , $\kappa_{1,2,3}$ change nonmonotonically and all approach zero when \tilde{U}_I is large, indicating a vanishing reaction rate in the extremely large U_I limit.

Equation 6 is universal for any particle number and any short-range interactions with arbitrary interaction strengths, as well as any real external potential. It separates C_{ν} , which fully capture the many-body physics, from two-body parameters, κ_{ν} , which are independent on the particle number and the temperature. Therefore, even when microscopic details of the reactive interaction, for instance, the exact expression of $U(\mathbf{r})$, are unknown, κ_{ν} can still be accessed in systems whose C_{ν} are easily measurable (Supplementary Materials). Equation 6 also holds for any many-body eigenstates, and a thermal average does not change its form. Therefore, Eq. 6

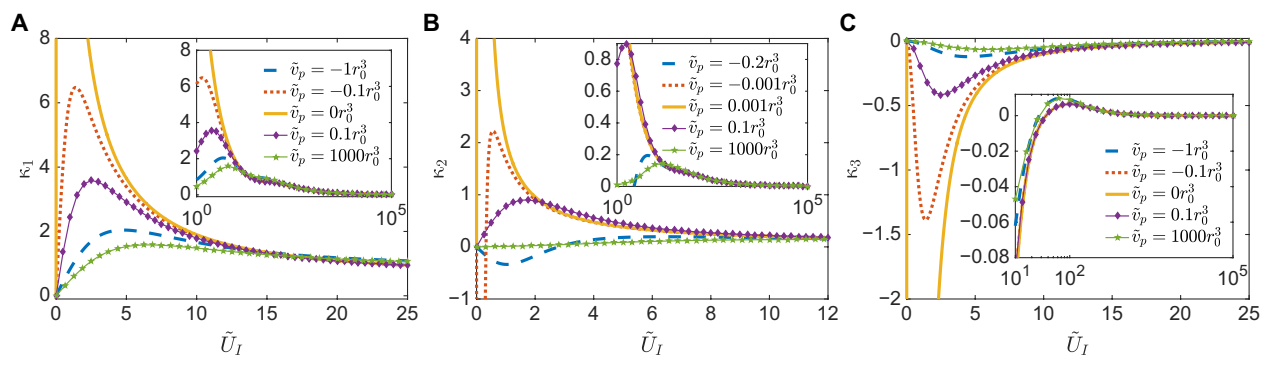


Fig. 2. Dependence of the three microscopic parameters on interactions. (**A** to **C**) ∇_p represents the scattering volume when $U_l = 0$. U_l is in the unit of $\hbar^2 / \left(M r_0^2\right)$. $\kappa_{1,2,3}$ are in the unit of r_0^{-3} , r_0^{-1} , and r_0^{-1} , respectively. When ∇_p crosses zero, the location of the maximum of κ_1 (κ_3) first approaches and then leaves the origin, and κ_1 (κ_3) remains positive (negative). In contrast, κ_2 quickly changes from positive to negative at small values of U_l when ∇_p crosses zero. In the large U_l limit, all three parameters vanish, as shown by the insets.

does apply for any finite temperatures, provided that the reaction rate is slow compared to the time scale of establishing quasi-equilibrium in the many-body system, i.e., the many-body system has a well-defined temperature at any time. Under this situation, C_v should be understood as their thermal averages.

We have found that κ_1 and κ_2 can be rewritten as familiar parameters. $\kappa_1 = \operatorname{Im}\left(v_p^{-1}\right)$ and $\kappa_2 = \operatorname{Im}\left[-1/(2r_e)\right]$ (Materials and Methods). In contrast, to our best knowledge, κ_3 is a new parameter that has not been addressed in previous works. Similar to κ_2 , κ_3 can be expressed as the difference between the extrapolation of the two-body wave function in the regime $|\mathbf{r}| > r_0$ toward the origin and the realistic wave function at short distance, $|\mathbf{r}| < r_0$ (Materials and Methods). Equation 6 can be rewritten as

$$\partial_t N = -\frac{\hbar}{8\pi^2 M} \left[\text{Im} \left(v_p^{-1} \right) C_1 - \frac{1}{2} \text{Im} \left(r_e^{-1} \right) C_2 + \kappa_3 C_3 \right]$$
 (13)

For s-wave inelastic scatterings due to complex zero-range interactions, the first term on the right-hand side of Eq. 13 was previously derived, with ν_p replaced by the complex s-wave scattering length (26). For a generic short-range interaction, all three contacts and all three microscopic parameters are required, as shown in Eqs. 6 and 13. In particular, when $\kappa_{2,3}$ are comparable to or even larger than κ_1 , the other two terms cannot be ignored. This expression allows us to directly connect the two-body loss rate to a wide range of physical quantities.

Universal relations with other physical quantities

We first consider the momentum distribution, which has a universal behavior when $|\mathbf{k}| \ll 1/r_0$ but is much larger than all other momentum scales, including k_F , the inverses of the scattering length and the thermal wavelength. We define the total angular averaged momentum, $n(|\mathbf{k}|) = \sum_{m=0,\pm 1} \int d\Omega n_m(\mathbf{k})$, where Ω is the solid angle

$$n(|\mathbf{k}|) \to \frac{C_1}{|\mathbf{k}|^2} \tag{14}$$

Once $n(|\mathbf{k}|)$ is measured, the first term in Eqs. 6 and 13 is known. For radio frequency (RF) spectroscopy in molecules, similar to that for atoms, Eq. 14 also indicates that such spectroscopy has a univer-

sal tail, $\Gamma(\omega) \rightarrow [(\Omega_{RF} V)/(8\pi^2)] C_1 (\hbar \omega/M)^{-1/2}$, where ω is the RF frequency, Ω_{RF} is the RF Rabi frequency, and V is the volume of the system. It is worth mentioning that, for atoms with elastic p-wave interactions, Eq. 14 describes the leading term of the large momentum tail (28-31). We have not found that the subleading term $\sim |\mathbf{k}|^{-4}$ has connections to two-body losses.

Another fundamentally important quantity in condensed matter physics is the density correlation function, $S(\mathbf{r}) = \int d\mathbf{R} \langle n(\mathbf{R} + \mathbf{r}/2)n(\mathbf{R} - \mathbf{r}/2) \rangle$, which measures the probability of having two particles separated by a distance \mathbf{r} . Using Eqs. 3 to 5, $S(\mathbf{r})$ can be evaluated explicitly in the regime, $r_0 < |\mathbf{r}| \ll k_F^{-1}$. To enhance the signal-to-noise ratio, $S(\mathbf{r})$ can be integrated over a shell with inner and outer radii, x and x + D, respectively. Such an integrated density correlation is given by $P(x,D) = \int_x^{x+D} d\mathbf{r} S(\mathbf{r})$, and

$$\frac{\partial P(x,D)}{\partial D}\Big|_{D\to 0} = \frac{1}{16\pi^2} \left\{ C_1 \frac{1}{x^2} + \frac{1}{2} C_2 - \left[2\operatorname{Re}\left(\frac{1}{\nu_p}\right) C_1 - \operatorname{Re}\left(\frac{1}{r_e}\right) C_2 + \operatorname{Im}\left(\frac{1}{r_e}\right) C_3 \right] \frac{x}{3} \right\} \tag{15}$$

Again, other partial waves have been suppressed in the expression, as their contributions are given by different spherical harmonics. Fitting $\partial P(x,D)/\partial D\mid_{D\to 0}$ measured in experiments using the power series in Eq. 15 allows one to obtain all three contacts, $C_{1,2,3}$, provided that v_p and r_e are known. If these two parameters are unknown, then it is necessary to include higher-order terms in the expansion (Materials and Methods).

We emphasize that, no matter whether thermodynamic quantities and correlation functions can be computed accurately in theories, Eqs. 6 and 13 to 15 allow experimentalists to explore how contacts determine chemical reactions in interacting few-body and many-body systems. In the strongly interacting regime where exact theoretical results are not available, these universal relations become most powerful.

Temperature dependence of the loss rate

It is useful to illuminate our results using some examples. For a two-body system in free space, the center of mass and the relative motion are decoupled. ϵ in Eqs. 7 to 9 becomes a good quantum number, i.e., $G(\mathbf{R}_{ij}; E - \epsilon)$ becomes a delta function in the energy space. For scattering states with $\epsilon > 0$, we consider the wave function,

 $\Psi^{[2]}(\mathbf{r}_1, \mathbf{r}_2) = \phi_c(\mathbf{R}_{12}) \psi(\mathbf{r}_{12})$, where $\phi_c(\mathbf{R}_{12})$ is a normalized wavefunction of the center of mass and $\psi(\mathbf{r}_{12}) = \sqrt{8\pi/V} [i/(\cot \eta - i)] [\cot \eta j_1 (q_\epsilon|\mathbf{r}_{12}|) - n_1(q_\epsilon|\mathbf{r}_{12}|)] \sum_m Y_{1m}(\hat{\mathbf{r}}_{12})$. Figure 3 shows the dependence of C_1 on \tilde{U}_I when \tilde{v}_p is fixed at various values. Results for a bound state are also shown. With increasing \tilde{U}_I , C_1 approaches a nonzero constant in both cases. Here, $C_2 = 2 C_1 \operatorname{Re} \left(q_\epsilon^2 \right)$. $C_3 = 0$ if we consider a scattering state. In contrast, $C_3 = 2 C_1 \operatorname{Im} \left(q_\epsilon^2 \right)$ for a bound state. Analytical results in the limits, $v_p = 0^\pm$, ∞ , are shown in Table 1.

We use the second-order virial expansion to study a thermal gas at high temperatures. The partition function is written as $Z=Z_0+e^{2\mu/(k_BT)}\sum_{E_c,n}(e^{-(E_c+\epsilon_n)/(k_BT)}-e^{-(E_c+\epsilon_n^0)/(k_BT)})$, where Z_0 is the partition function of noninteracting fermions, μ is the chemical potential, and $E_c=\hbar^2K^2/(4M)$ is the energy of the center of mass motion carrying a momentum K. ϵ_n and ϵ_n^0 are the eigenenergies of the relative motion with and without interactions, respectively. On the basis of the results of the two-body problem, thermal averaged contacts are derived using $\langle C_v \rangle_T = Z^{-1}e^{2\mu/(k_BT)}(\Sigma_{E_c}e^{-E_c/(k_BT)})(\Sigma_n C_v(\epsilon_n)e^{-\epsilon_n/(k_BT)})$. Using $N=k_BT\partial_\mu \ln Z$, we eliminate μ and obtain $\langle C_{v/T}$ as a function of N and T. Analytical expressions in the limits, $v_p=0^\pm,\infty$, are shown in Table 2.

Table 2 may shed light on some recent experiments conducted in the weakly interacting regime (9, 12). Although $v_p > 0$, it is likely that bound states are not occupied, i.e., the system is prepared at the upper branch. Therefore, $C_3 = 0$. In a homogenous system, we obtain

$$\partial_{t} N = \frac{144 \pi^{2}}{h} \operatorname{Im}(v_{p}) N n k_{B} T + \frac{360 \pi^{2}}{h} \operatorname{Im}\left(\frac{v_{p}}{v_{p}^{*}} r_{e}^{-1}\right) \frac{M |v_{p}|^{2}}{\hbar^{2}} N n k_{B}^{2} T^{2}$$
(16)

A previous work derived the first term in Eq. 16 using a different approach (22). However, a complete expression needs to include the contribution from r_e , which leads to a different power of the dependence on T. A recent experiment has shown the deviation from the linear dependence on T (12). However, it is worth investigating whether such deviation comes from the second term in Eq. 16 or some other effects, particularly correlations beyond the description of the second-order virial expansion.

As a harmonic trap exists in experiments, the dependence on T could be completely different. We use the local density approximation to obtain the total contacts by integrating local contacts. As a result, $C_v^{\text{trap}} = \left[(\pi k_{\text{B}} T)/(M\omega^2) \right]^{3/2} C_v(0)$, where ω is trapping fre-

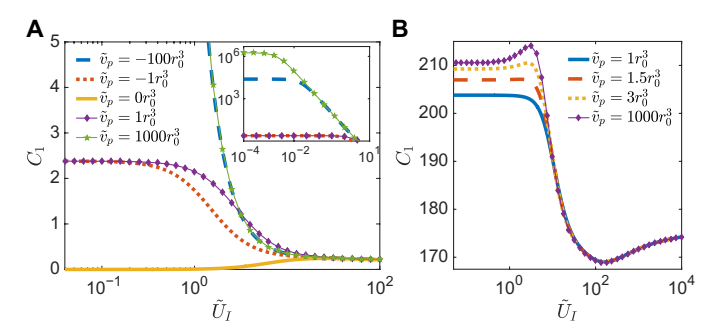


Fig. 3. Contacts of a two-body system. (**A**) C_1 (in the unit of r_0^4/V) of a scattering state as a function of \tilde{U}_I [in the unit of $\hbar^2/(Mr_0^2)$] when \tilde{v}_p is fixed at various values. $q_{\epsilon} = 0.01/r_0$. (**B**) C_1 (in the unit of r_0) of a bound state as a function of \tilde{U}_I [in the unit of $\hbar^2/(Mr_0^2)$].

Table 1. Analytical expressions for contacts C_v **of two particles in different limits.** Lines 1 and 2 show the results in the weakly interacting regime and those at resonance, respectively. $v_p \rightarrow 0_{\pm}$ (∞) means $v_p \rightarrow 0_{\pm} + 0i$ ($\infty + 0i$) on the complex plane. Line 3 includes the results for bound states, in which a single angular momentum m is considered.

\mathbf{v}_p	C ₁	C ₂	C ₃
$v_p \rightarrow 0_{\pm}$	$12(4\pi)^3 q_{\epsilon}^2 v_p ^2 / V$	$2C_1\operatorname{Re}(q_{\epsilon}^2)$	0
$V_p \rightarrow \infty$	$12(4\pi)^3 q_{\epsilon}^{-2} r_{\epsilon} ^2/V$	$2C_1\operatorname{Re}(q_{\epsilon}^2)$	0
Bound	$2(4\pi)^2 \text{ Re } (-r_e)$	$2C_1\operatorname{Re}ig(q_{\epsilon}^2ig)$	$2C_1\operatorname{Im}(q_{\epsilon}^2)$

quency and $C_{\nu}(0)$ are the contact densities at the center of the trap (Supplementary Materials). Consequently

$$\partial_{t} N^{\text{trap}} = \frac{18\sqrt{\pi}}{h} (M\omega^{2})^{\frac{3}{2}} \text{Im}(\nu_{p}) (N^{\text{trap}})^{2} \frac{1}{\sqrt{k_{\text{B}}T}} + \frac{45\sqrt{\pi}}{h} (M\omega^{2})^{\frac{3}{2}} \text{Im} \left(\frac{\nu_{p}}{\nu_{p}^{*}} r_{e}^{-1}\right) \frac{M|\nu_{p}|^{2}}{\hbar^{2}} (N^{\text{trap}})^{2} \sqrt{k_{\text{B}}T}$$
(17)

The first term decreases with increasing T, in sharp contrast to the homogeneous case. In a trap, the molecular cloud expands when the temperature increases such that densities and the total contacts decrease for a fixed N. Similarly, the second term increases slower than the result in homogeneous systems with increasing T. Alternatively, we could consider the density at the center of the trap, the decay rate of which linearly depends on T again (Supplementary Materials). Whereas the temperature dependence of the loss rate in the trap can be qualitatively obtained from the result in a homogenous system by considering a temperature-dependent volume $\sim T^{3/2}$ (12), a rigorous calculation as aforementioned is required to obtain the exact numerical factors in Eq. 17.

DISCUSSION

Although we have used the high-temperature regime as an example to explain Eqs. 6 and 13 to 15, we need to emphasize that these universal relations are powerful tools at any temperatures. In particular, at lower temperatures, contacts are no longer proportional to N^2 , directly reflecting the critical roles of many-body correlations in determining the reaction rate. For instance, below the superfluid transition temperature, contacts may be directly related to superfluid-order parameters (32, 33). Universal relations constructed here thus offer us a unique means to explore the interplay between the chemical reaction and symmetry breaking in quantum many-body systems.

We also would like to point out that the density fluctuation measured in experiments (12, 14), $f(\mathbf{r}_s) = \langle n^2(\mathbf{r}_s) \rangle - \langle n(\mathbf{r}_s) \rangle^2$, is different from the density-density correlation, $S(\mathbf{r})$, studied in our work. Whereas $S(\mathbf{r})$ directly tells us all contacts by capturing the probability of having two particles as a function of \mathbf{r} , their relative coordinate, $f(\mathbf{r}_s)$ traces the compressibility $\partial n/\partial \mu$ as a function of \mathbf{r}_s , the single-particle coordinate. Since the pressure, P, is controlled by contacts and other thermodynamical quantities can be derived from P(34), how the compressibility and $f(\mathbf{r}_s)$ are related to contacts

Table 2. Analytical expressions for thermal averaged contacts $(C_v)_T$ in different limits. Lines 1 and 2 show the results in the weakly interacting regime. When v_p is positive, bound states exist and their contributions are included in line 1. Line 3 includes the results at resonance. N_D is the number of dimers. $\lambda_T = [(2\pi\hbar^2)/(Mk_BT)]^{1/2}$ is the thermal wavelength.

v_p	$\langle C_1 \rangle_T$	$\langle C_2 \rangle_{\mathcal{T}}$	⟨ C ₃ ⟩ _T
$v_p \rightarrow 0_+$	72 $(2\pi)^4 v_p ^2 \lambda_T^{-2} Nn$ +2 $(4\pi)^2 \text{Re}(-r_e) N_D$	360 $(2\pi)^5 v_p ^2 \lambda_T^{-4} Nn$ +4 $(4\pi)^2 \operatorname{Re}(-r_e) \operatorname{Re}(r_e/v_p) N_D$	$4 \left(4\pi\right)^2 \operatorname{Re}(-r_e) \operatorname{Im}\left(r_e/v_p\right) N_D$
$v_p \rightarrow 0$	$72(2\pi)^4 v_p ^2 \lambda_T^{-2} Nn$	$360(2\pi)^5 v_p ^2 \lambda_T^{-4} Nn$	0
$V_p \rightarrow \infty$	$24\left(4\pi\right)^{2}\left r_{e}\right ^{2}\lambda_{T}^{2}Nn$	$12(4\pi)^3 r_e ^2 Nn$	0

and the loss rate remains an interesting open question worthy of exploration.

In current experiments (12, 14), the electric field is absent and the unpolarized molecules interact with each other with the van der Waals potential. Once an electric field is turned on, the dipoledipole interaction between polarized molecules, $\sim 1/|\mathbf{r}|^3$, decays slower and has a longer range. For any power-law potentials, $A/|\mathbf{r}|^n$, if n > 2, then the scattering theory applies and a characteristic length of the range of the interaction can be defined as \tilde{r} $(M|A|/\hbar^2)^{1/(n-2)}$ (35). In dilute systems, once $k_F \tilde{r} \ll 1$ is satisfied, universal relations rise from such a length scale separation. The details of the interaction, such as n of the power-law potential, determine the low energy expansion of the phase shift and microscopic parameters in the universal relations. It will be interesting to study how the electric field influences contacts, universal relations, and the decay rate of molecules. It is also worth mentioning a subtlety in the p-wave scattering when n = 6. It has been theoretically predicted that an extra term linearly dependent on the momentum should exist in the phase shift (36, 37). Whereas current experiments have not found evidence for extra contacts associated with this term yet (31), it will be useful to explore whether such a term may affect contacts, chemical reactions, and any other observables in many-body systems.

In addition to macroscopic systems, multibody correlations can also be studied in mesoscopic traps with controllable particle numbers. For instance, a recent experiment has found that the loss rate in a deep optical lattice, where each lattice site traps a few molecules, deviates substantially from the result in a large trap (38). Optical tweezers have also been implemented to study quantum effects in collisions or chemical reactions of a few particles (39, 40). Contacts of these few-body systems may be evaluated exactly and thus provide us with quantitative results of how multibody correlations determine two-body collisions and quantum chemical reactions.

More broadly, our results unfold intriguing universality in non-Hermitian systems. Recently, there have been extensive interest in studying open systems, where very rich non-Hermitian phenomena have been identified (41, 42). However, most of these studies have been focusing on either noninteracting systems or the weakly interacting regime where perturbative or mean-field approaches apply. Universal relations derived here are valid for any interaction strengths and thus deliver a unique tool to tackle interacting non-Hermitian systems and to unfold possible universal behaviors behind the complexity in quantum systems coupled to environment. We hope that our work will stimulate more studies of con-

tacts and universal relations to bridge quantum chemistry; atomic, molecular, and optical physics; and condensed matter physics.

MATERIALS AND METHODS

The Lindblad equation

We consider a Lindblad master equation

$$\hbar \frac{d\rho}{dt} = -i[H, \rho] + \mathcal{D}[\rho]$$
 (18)

where H is the Hamiltonian that describes the unitary part of the time evolution and the dissipator \mathcal{D} describes the loss due to inelastic collisions

$$\mathcal{D}[\rho] = -\int d\mathbf{x}_1 d\mathbf{x}_2 \frac{1}{2} \Gamma(|\mathbf{x}_1 - \mathbf{x}_2|) \left(2\Psi(\mathbf{x}_2) \Psi(\mathbf{x}_1) \rho \Psi^{\dagger}(\mathbf{x}_1) \Psi^{\dagger}(\mathbf{x}_2) - \left\{ \Psi^{\dagger}(\mathbf{x}_1) \Psi^{\dagger}(\mathbf{x}_2) \Psi(\mathbf{x}_2) \Psi(\mathbf{x}_1), \rho \right\} \right)$$
(19)

 $\Psi(\mathbf{x})$ is the fermionic field operator satisfying $\{\Psi(\mathbf{x}), \Psi^{\dagger}(\mathbf{x}')\} = \delta^{(3)}(\mathbf{x} - \mathbf{x}')$. $(1/2)\Gamma(|\mathbf{x}_1 - \mathbf{x}_2|)$ describes a finite range dissipation. The loss rate of the total particle number, $dN/dt = \int d\mathbf{x} (d/dt) \operatorname{Tr}(n(\mathbf{x})\rho)$, $n(\mathbf{x}) = \Psi^{\dagger}(\mathbf{x})\Psi(\mathbf{x})$, is written as

$$\frac{dN}{dt} = -\frac{1}{\hbar} \text{Tr} \left(\int d\mathbf{x} \Psi^{\dagger}(\mathbf{x}) \Psi(\mathbf{x}) \int d\mathbf{x}_{1} d\mathbf{x}_{2} \frac{1}{2} \Gamma(|\mathbf{x}_{1} - \mathbf{x}_{2}|) \right) \\
\times \left[2\Psi(\mathbf{x}_{2}) \Psi(\mathbf{x}_{1}) \rho \Psi^{\dagger}(\mathbf{x}_{1}) \Psi^{\dagger}(\mathbf{x}_{2}) - \left\{ \Psi^{\dagger}(\mathbf{x}_{1}) \Psi^{\dagger}(\mathbf{x}_{2}) \Psi(\mathbf{x}_{2}) \Psi(\mathbf{x}_{1}), \rho \right\} \right] \right) \\
= -\frac{1}{\hbar} \int d\mathbf{x}_{1} d\mathbf{x}_{2} d\mathbf{x} \Gamma(|\mathbf{x}_{1} - \mathbf{x}_{2}|) \text{Tr} \left(\rho \left[\Psi^{\dagger}(\mathbf{x}_{1}) \Psi^{\dagger}(\mathbf{x}_{2}), \Psi^{\dagger}(\mathbf{x}_{2}), \Psi^{\dagger}(\mathbf{x}_{2}) \Psi(\mathbf{x}_{1}) \right] \\
\Psi^{\dagger}(\mathbf{x}) \Psi(\mathbf{x}) \Psi(\mathbf{x}_{2}) \Psi(\mathbf{x}_{1}) \right) \\
= \frac{2}{\hbar} \int d\mathbf{x} d\mathbf{x}' \Gamma(|\mathbf{x}' - \mathbf{x}|) \langle \Psi^{\dagger}(\mathbf{x}) \Psi^{\dagger}(\mathbf{x}') \Psi(\mathbf{x}') \Psi(\mathbf{x}) \rangle$$
(20)

This equation is valid for any finite range dissipator. In the approximation of zero-range dissipators, $\Gamma = g\delta^{(3)}(\mathbf{x} - \mathbf{x}')$, it reduces to (43–45)

$$\frac{dN}{dt} = \frac{2}{\hbar} g \int d\mathbf{x} \langle \Psi^{\dagger}(\mathbf{x}) \Psi^{\dagger}(\mathbf{x}) \Psi(\mathbf{x}) \Psi(\mathbf{x}) \rangle$$
 (21)

The work in (43) considered two-component fermions and obtained $d\langle N_1\rangle/dt = d\langle N_2\rangle/dt = -\left[\hbar/(2\pi m)\right] \text{ Im } (1/a)C$, where N_1 (N_2) is the number of spin-up (spin-down) fermions, a is the s-wave scattering length, and C is the s-wave contact.

We emphasize that Eq. 20 is equivalent to results derived from the Hamiltonian with a complex interaction, as shown in Eq. 24 in the next section, provided that we identify U_I and Γ , i.e., $U_I(|\mathbf{x}' - \mathbf{x}|) = \Gamma(|\mathbf{x}' - \mathbf{x}|)$. Thus, universal relations derived from the Lindblad equation are the same as those shown here since the probability of having more than two particles within a distance smaller than r_0 is negligible in dilute systems satisfying $r_0 \ll k_F^{-1}$.

Decay rate

In the presence of complex short-range interactions, the many-body wave function satisfies

$$i\hbar \partial_t \Psi(\mathbf{r}_1, \mathbf{r}_2, ..., \mathbf{r}_N) = \left[\sum_{i=1}^N \left[-\frac{\hbar^2}{2M} \nabla_i^2 + V_{\text{ext}}(\mathbf{r}_i) \right] + \sum_{i>j} U(\mathbf{r}_{ij}) \right] \Psi(\mathbf{r}_1, \mathbf{r}_2, ..., \mathbf{r}_N)$$
(22)

For any finite-size system, net current vanishes at the boundary. We obtain

$$\partial_t N = \frac{4}{\hbar} \sum_{i>j} \int d\mathbf{R}_{ij} d\mathbf{r}_{ij} U_I(\mathbf{r}_{ij}) |\Psi(\mathbf{R}_{ij}, \mathbf{r}_{ij})|^2$$
 (23)

which is equivalent to a second quantization form using fermionic operators

$$\partial_t N = \frac{2}{\hbar} \int d\mathbf{x} d\mathbf{x}' \, U_I(|\mathbf{x}' - \mathbf{x}|) \langle \Psi^{\dagger}(\mathbf{x}) \, \Psi^{\dagger}(\mathbf{x}') \, \Psi(\mathbf{x}') \, \Psi(\mathbf{x}) \rangle \quad (24)$$

Using Eq. 3 and $\epsilon \psi_m(\mathbf{r}_{ij}; \epsilon) = [-(\hbar^2/M) \nabla_{r_{ij}}^2 + U(\mathbf{r}_{ij})] \psi_m(\mathbf{r}_{ij}; \epsilon)$, we obtain

$$2i\sum_{j>i}\int d\mathbf{R}_{ij}\int_{0}^{r_{0}}d\mathbf{r}_{ij} |\Psi(\mathbf{R}_{ij},\mathbf{r}_{ij})|^{2}U_{I}(\mathbf{r}_{ij})$$

$$-\sum_{j>i}\int d\mathbf{R}_{ij}\int_{0}^{r_{0}}d\mathbf{r}_{ij} [\Psi^{*}(\mathbf{R}_{ij},\mathbf{r}_{ij})$$

$$\times\sum_{m,\epsilon}\epsilon G_{m}(\mathbf{R}_{ij};E-\epsilon)\psi_{m}(\mathbf{r}_{ij};\epsilon)]$$

$$+\sum_{j>i}\int d\mathbf{R}_{ij}\int_{0}^{r_{0}}d\mathbf{r}_{ij} [\Psi(\mathbf{R}_{ij},\mathbf{r}_{ij})$$

$$\times\sum_{m,\epsilon}\epsilon^{*}G_{m}^{*}(\mathbf{R}_{ij};E-\epsilon)\psi_{m}^{*}(\mathbf{r}_{ij};\epsilon)]$$

$$=\frac{\hbar^{2}}{M}\sum_{j>i}\int d\mathbf{R}_{ij}\int_{0}^{r_{0}}d\mathbf{r}_{ij} [\Psi^{*}(\mathbf{R}_{ij},\mathbf{r}_{ij})\nabla_{r_{ij}}^{2}\Psi(\mathbf{R}_{ij},\mathbf{r}_{ij})$$

$$-\Psi(\mathbf{R}_{ij},\mathbf{r}_{ij})\nabla_{r_{ij}}^{2}\Psi^{*}(\mathbf{R}_{ij},\mathbf{r}_{ij})]$$

Note that, for the system with isotropic interactions $U(\mathbf{r}) = U(|\mathbf{r}|)$ and $\psi_m(\mathbf{r}_{ij}; \epsilon) = \varphi(|\mathbf{r}_{ij}|; \epsilon) Y_{1m}(\hat{\mathbf{r}}_{ij})$, one has (29)

$$v_p = \frac{r_0^3}{3} \frac{r_0 \,\varsigma - 2}{r_0 \,\varsigma + 1} \tag{26}$$

$$\frac{1}{r_e} = -\frac{1}{r_0} - \frac{r_0^2}{3} \frac{1}{v_p} + \frac{r_0^5}{45} \frac{1}{(v_r)^2} - \int_0^{r_0} \left[\varphi^{(0)}(r) \right]^2 r^2 dr \tag{27}$$

where $\varsigma = \{\partial \ln [r\varphi(r;\epsilon)]/\partial r\}|_{\epsilon=0}$. On the basis of Eqs. 4, 5, and 27, we define $C_{1m}^{ss'} = (4\pi)^2 N(N-1) \int d\mathbf{R}_{ij} g_m^{(s)*} g_m^{(s)*}, g_m^{(s)} = \Sigma_\epsilon q_\epsilon^{2s} G_m(\mathbf{R}_{ij};E-\epsilon)$, and $C_{1m} = C_{1m}^{00}$ and obtain

$$\sum_{m} \left[\operatorname{Im} \left(- v_{p}^{-1} \right) C_{1m} + \frac{1}{2} \operatorname{Im} \left(r_{e}^{-1} \right) \left(C_{1m}^{01} + C_{1m}^{10} \right) \right. \\
\left. - i \kappa_{3} \left(C_{1m}^{01} - C_{1m}^{10} \right) + \operatorname{O} \left(\left(E - E^{*} \right)^{2} \right) \right] \\
= \frac{(4\pi)^{2} 2M}{\hbar^{2}} \sum_{i>j} \int d\mathbf{R}_{ij} \int_{0}^{r_{0}} d\mathbf{r}_{ij} \left| \sum_{m,\epsilon} G_{m} \left(\mathbf{R}_{ij}; E - \epsilon \right) \psi_{m} \left(\mathbf{r}_{ij}; \epsilon \right) \right|^{2} U_{I}(\mathbf{r}_{ij}) \tag{28}$$

which leads to Eqs. 10 to 12,

$$\kappa_{1} = \operatorname{Im}\left(v_{p}^{-1}\right) = -\frac{M}{\hbar^{2}} \int_{0}^{\infty} dr r^{2} \left|\phi^{(0)}(r)\right|^{2} U_{I}(r) \tag{29}$$

$$\kappa_{2} = \operatorname{Im}\left(-r_{e}^{-1}/2\right) = -\frac{M}{\hbar^{2}} \operatorname{Re}\left(\int_{0}^{\infty} dr r^{2} \phi^{(0)*}(r) \phi^{(1)}(r) U_{I}(r)\right) \tag{30}$$

$$\kappa_{3} = -\int_{0}^{r_{0}} \left\{ \left[\operatorname{Im}\phi^{(0)}(r)\right]^{2} - \left[\operatorname{Im}\widetilde{\phi}^{(0)}(r)\right]^{2} \right\} r^{2} dr$$

$$\kappa_{3} = -J_{0} \{ [\operatorname{Im} \varphi^{(r)}] - [\operatorname{Im} \varphi^{(r)}] \} r dr
= \frac{M}{\hbar^{2}} \operatorname{Im} \left(\int_{0}^{\infty} dr r^{2} \varphi^{(0)} (r) \varphi^{(1)}(r) U_{I}(r) \right)$$
(31)

where $\tilde{\varphi}^{(0)}(r)$ is a wave function obtained from extending the actual wave function $\varphi^{(0)}(r)$ outside the potential $(r > r_0)$ into the regime $r < r_0$. We obtain Eq. 13

$$\partial_t N = -\frac{\hbar}{8\pi^2 M} \left[\text{Im} \left(v_p^{-1} \right) C_1 - \frac{1}{2} \text{Im} \left(r_e^{-1} \right) C_2 + \kappa_3 C_3 \right]$$
 (32)

where $C_1 = \Sigma_m C_{1m}$, $C_2 = 2 \sum_m \text{Re} \left(C_{1m}^{01} \right)$, and $C_3 = 2 \sum_m \text{Im} \left(C_{1m}^{01} \right)$. The above equation leads to Eqs. 7 to 9 by considering $G_m(\mathbf{R}_{ij}; E - \epsilon) = G(\mathbf{R}_{ij}; E - \epsilon)$.

Momentum distribution

Similar to systems with real interactions (30), using $n(\mathbf{k}) = \sum_{i=1}^{N} \int \prod_{j \neq i} d\mathbf{r}_{i} ||\mathbf{d}\mathbf{r}_{i} || ||$

$$n(\mathbf{k}) \xrightarrow{k_F \ll |\mathbf{k}| \ll r_0^{-1}} \frac{C_1}{3|\mathbf{k}|^2} \sum_{m} |Y_{1m}(\widehat{\mathbf{k}})|^2$$
(33)

which leads to

$$n(|\mathbf{k}|) = \int d\Omega n(\mathbf{k}) = \frac{C_1}{|\mathbf{k}|^2}$$
 (34)

Density correlations

The density correlation function $S(\mathbf{r}) = \int d\mathbf{R} \langle n(\mathbf{R} + \mathbf{r}/2) n(\mathbf{R} - \mathbf{r}/2) \rangle$ can be rewritten as

$$S(\mathbf{r}) = N(N-1) \int (\prod_{k \neq i,j} d\mathbf{r}_k) \times \left| \Psi \left(\mathbf{r}_1, ..., \mathbf{r}_i = \mathbf{R} + \frac{\mathbf{r}}{2}, ..., \mathbf{r}_j = \mathbf{R} - \frac{\mathbf{r}}{2}, ..., \mathbf{r}_N \right) \right|^2$$
(35)

In the regime, $r \ll k_F^{-1}$, $S(\mathbf{r})$ is written as

$$S(\mathbf{r}) = N(N-1) \int d\mathbf{R}_{ij} \sum_{m} |Y_{1m}(\hat{\mathbf{r}})|^2 [|\phi_m^{(0)}(r)|^2 |g_m^{(0)}|^2 + \phi_m^{(0)}(r) \phi_m^{(1)*}(r) g_m^{(1)*} g_m^{(0)} + \phi_m^{(1)}(r) \phi_m^{(0)*}(r) g_m^{(0)*} g_m^{(1)}]$$
(36)

where $r = |\mathbf{r}|$. The integral over a shell allows us to obtain

$$P(x,D) = \int_{x}^{x+D} d\mathbf{r} S(\mathbf{r}) = \frac{1}{(4\pi)^{2}} \sum_{m} \int_{x}^{x+D} r^{2} dr \Big[\varphi_{m}^{(0)}(r) \varphi_{m}^{(0)*}(r) C_{1m} + \varphi_{m}^{(0)}(r) \varphi_{m}^{(1)*}(r) C_{1m}^{10} + \varphi_{m}^{(1)}(r) \varphi_{m}^{(0)*}(r) C_{1m}^{01} \Big]$$
(37)

Using Eqs. 4 and 5, we obtain

$$\frac{\partial P(x,D)}{\partial D}\Big|_{D\to 0} = \frac{1}{16\pi^{2}} \left\{ C_{1} \frac{1}{x^{2}} + C_{2} \frac{1}{2} + \left[-2\operatorname{Re}\left(\frac{1}{v_{p}}\right) C_{1} + \operatorname{Re}\left(\frac{1}{r_{e}}\right) C_{2} - \operatorname{Im}\left(\frac{1}{r_{e}}\right) C_{3} \right] \frac{x}{3} + \left[-\frac{2}{3}\operatorname{Re}\left(\frac{1}{v_{p}}\right) C_{2} - \operatorname{Im}\left(\frac{1}{v_{p}}\right) C_{3} \right] \frac{x^{3}}{5} + \left[\frac{1}{|v_{p}|^{2}} C_{1} - \operatorname{Re}\left(\frac{1}{v_{p}^{*}} r_{e}\right) C_{2} + \operatorname{Im}\left(\frac{1}{v_{p}^{*}} r_{e}\right) C_{3} \right] \frac{x^{4}}{9} - \frac{C_{2}}{90 |v_{p}|^{2}} x^{6} \right\}$$
(38)

where the first line recovers Eq. 15 and the second line includes higher-order terms. When v_p and r_e are known, the first line readily allows experimentalists to obtain $C_{1,2,3}$ by fitting the experimental data. When v_p and r_e are unknown, the second line is required to obtain C_v , v_p , and r_e .

SUPPLEMENTARY MATERIALS

Supplementary material for this article is available at http://advances.sciencemag.org/cgi/content/full/6/51/eabd4699/DC1

REFERENCES AND NOTES

- K.-K. Ni, S. Ospelkaus, M. H. G. de Miranda, A. Pe'er, B. Neyenhuis, J. J. Zirbel, S. Kotochigova, P. S. Julienne, D. S. Jin, J. Ye, A high phase-space-density gas of polar molecules. *Science* 322, 231–235 (2008).
- J. Deiglmayr, A. Grochola, M. Repp, K. Mörtlbauer, C. Glück, J. Lange, O. Dulieu, R. Wester, M. Weidemüller, Formation of ultracold polar molecules in the rovibrational ground state. *Phys. Rev. Lett.* 101, 133004 (2008).
- P. K. Molony, P. D. Gregory, Z. H. Ji, B. Lu, M. P. Köppinger, C. R. Le Sueur, C. L. Blackley, J. M. Hutson, S. L. Cornish, Creation of ultracold ⁸⁷Rb¹³³Cs molecules in the rovibrational ground state. *Phys. Rev. Lett.* **113**. 255301 (2014).
- T. Takekoshi, L. Reichsöllner, A. Schindewolf, J. M. Hutson, C. R. Le Sueur, O. Dulieu, F. Ferlaino, R. Grimm, H.-C. Nägerl, Ultracold dense samples of dipolar rbcs molecules in the rovibrational and hyperfine ground state. *Phys. Rev. Lett.* 113, 205301 (2014).
- T. Shimasaki, M. Bellos, C. D. Bruzewicz, Z. Lasner, D. DeMille, Production of rovibronicground-state RbCs molecules via two-photon-cascade decay. *Phys. Rev. A* 91, 021401 (2015).
- J. W. Park, S. A. Will, M. W. Zwierlein, Ultracold dipolar gas of fermionic ²³Na ⁴⁰K molecules in their absolute ground state. *Phys. Rev. Lett.* **114**, 205302 (2015).
- M. Y. Guo, B. Zhu, B. Lu, X. Ye, F. D. Wang, R. Vexiau, N. Bouloufa-Maafa, G. Quéméner, O. Dulieu, D. J. Wang, Creation of an ultracold gas of ground-state dipolar ²³Na⁸⁷Rb molecules. *Phys. Rev. Lett.* **116**, 205303 (2016).
- L. W. Cheuk, L. Anderegg, Y. C. Bao, S. Burchesky, S. Yu, W. Ketterle, K.-K. Ni, J. M. Doyle, Observation of collisions between two ultracold ground-state CaF molecules. *Phys. Rev. Lett.* 125, 043401 (2020).
- S. Ospelkaus, K.-K. Ni, D. Wang, M. H. G. de Miranda, B. Neyenhuis, G. Quéméner, P. S. Julienne, J. L. Bohn, D. S. Jin, J. Ye, Quantum-state controlled chemical reactions of ultracold potassium-rubidium molecules. *Science* 327, 853–857 (2010).
- X. Ye, M. Y. Guo, M. L. González-Martínez, G. Quéméner, D. J. Wang, Collisions of ultracold ²³Na⁸⁷Rb molecules with controlled chemical reactivities. Sci. Adv. 4, eaaq0083 (2018).
- P. D. Gregory, M. D. Frye, J. A. Blackmore, E. M. Bridge, R. Sawant, J. M. Hutson,
 L. Cornish, Sticky collisions of ultracold RbCs molecules. *Nat. Commun.* 10, 3104 (2019)
- L. De Marco, G. Valtolina, K. Matsuda, W. G. Tobias, J. P. Covery, J. Ye, A degenerate Fermi gas of polar molecules. Science 363, 853–856 (2019).
- M.-G. Hu, Y. Liu, D. D. Grimes, Y.-W. Lin, A. H. Gheorghe, R. Vexiau, N. Bouloufa-Maafa,
 O. Dulieu, T. Rosenband, K.-K. Ni, Direct observation of bimolecular reactions of ultracold KRb molecules. Science 366, 1111–1115 (2019).
- W. G. Tobias, K. Matsuda, G. Valtolina, L. De Marco, J.-R. Li, J. Ye, Thermalization and sub-Poissonian density fluctuations in a degenerate molecular fermi gas. *Phys. Rev. Lett.* 124, 033401 (2020).
- H. P. Büchler, E. Demler, M. Lukin, A. Micheli, N. Prokof'ev, G. Pupillo, P. Zoller, Strongly correlated 2D quantum phases with cold polar molecules: Controlling the shape of the interaction potential. *Phys. Rev. Lett.* 98, 060404 (2007).

- N. R. Cooper, G. V. Shlyapnikov, Stable topological superfluid phase of ultracold polar fermionic molecules. *Phys. Rev. Lett.* 103, 155302 (2009).
- N. Y. Yao, A. V. Gorshkov, C. R. Laumann, A. M. Läuchli, J. Ye, M. D. Lukin, Realizing fractional chern insulators in dipolar spin systems. *Phys. Rev. Lett.* 110, 185302 (2013)
- S. V. Syzranov, M. L. Wall, V. Gurarie, A. M. Rey, Spin-orbital dynamics in a system of polar molecules. Nat. Commun. 5, 5391 (2014).
- D. DeMille, Quantum computation with trapped polar molecules. Phys. Rev. Lett. 88, 067901 (2002).
- S. F. Yelin, K. Kirby, R. Côté, Schemes for robust quantum computation with polar molecules. *Phys. Rev. A* 74, 050301 (2006).
- M. Mayle, G. Quéméner, B. P. Ruzic, J. L. Bohn, Scattering of ultracold molecules in the highly resonant regime. *Phys. Rev. A* 87, 012709 (2013).
- Z. Idziaszek, P. S. Julienne, Universal rate constants for reactive collisions of ultracold molecules. *Phys. Rev. Lett.* **104**, 113202 (2010).
- S. Tan, Energetics of a strongly correlated Fermi gas. Ann. Phys. 323, 2952–2970 (2008)
- S. Tan, Large momentum part of a strongly correlated Fermi gas. Ann. Phys. 323, 2971–2986 (2008).
- S. Tan, Generalized virial theorem and pressure relation for a strongly correlated Fermi gas. Ann. Phys. 323, 2987–2990 (2008).
- E. Braaten, H.-W. Hammer, Universal relation for the inelastic two-body loss rate. J. Phys. B 46, 215203 (2013).
- S. Laurent, M. Pierce, M. Delehaye, T. Yefsah, F. Chevy, C. Salomon, Connecting few-body inelastic decay to quantum correlations in a many-body system: A weakly coupled impurity in a resonant Fermi gas. *Phys. Rev. Lett.* 118, 103403 (2017).
- S. M. Yoshida, M. Ueda, Universal high-momentum asymptote and thermodynamic relations in a spinless Fermi gas with a resonant p-wave interaction. Phys. Rev. Lett. 115, 135303 (2015).
- Z. H. Yu, J. H. Thywissen, S. Z. Zhang, Universal relations for a Fermi gas close to a p-wave interaction resonance. Phys. Rev. Lett. 115, 135304 (2015).
- M. Y. He, S. L. Zhang, H. M. Chan, Q. Zhou, Concept of a contact spectrum and its applications in atomic quantum Hall states. *Phys. Rev. Lett.* 116, 045301 (2016).
- C. Luciuk, S. Trotzky, S. Smale, Z. H. Yu, S. Z. Zhang, J. H. Thywissen, Evidence for universal relations describing a gas with p-wave interactions. Nat. Phys. 12, 599–605 (2016).
- S.-L. Zhang, M. Y. He, Q. Zhou, Contact matrix in dilute quantum systems. Phys. Rev. A 95, 062702 (2017).
- S. M. Yoshida, M. Ueda, p-wave contact tensor: Universal properties of axisymmetrybroken p-wave Fermi gases. Phys. Rev. A 94, 033611 (2016).
- T.-L. Ho, Q. Zhou, Obtaining the phase diagram and thermodynamic quantities of bulk systems from the densities of trapped gases. Nat. Phys. 6, 131–134 (2010).
- 35. H. Friedrich, Scattering Theory (Springer, 2013).
- 36. N. F. Mott, H. S. W. Massey, *The Theory of Atomic Collisions* (Clarendon, 1965).
- B. Gao, Quantum-defect theory of atomic collisions and molecular vibration spectra. *Phys. Rev. A* 58, 4222 (1998).
- A. Goban, R. B. Hutson, G. E. Marti, S. L. Campbell, M. A. Perlin, P. S. Julienne, J. P. D'Incao, A. M. Rey, J. Ye, Emergence of multi-body interactions in a fermionic lattice clock. *Nature* 563, 369–373 (2018).
- A. M. Kaufman, B. J. Lester, C. M. Reynolds, M. L. Wall, M. Foss-Feig, K. R. A. Hazzard, A. M. Rey, C. A. Regal, Two-particle quantum interference in tunnel-coupled optical tweezers. *Science* 345, 306–309 (2014).
- L. Anderegg, L. W. Cheuk, Y. Bao, S. Burchesky, W. Ketterle, K.-K. Ni, J. M. Doyle, An optical tweezer array of ultracold molecules. *Science* 365, 1156–1158 (2019).
- E. J. Bergholtz, J. C. Budich, F. K. Kunst, Exceptional Topology of Non-Hermitian Systems. arXiv:1912.10048 [cond-mat.mes-hall] (20 December 2019).
- K. Yamamoto, M. Nakagawa, K. Adachi, K. Takasan, M. Ueda, N. Kawakami, Theory of non-Hermitian fermionic superfluidity with a complex-valued interaction. *Phys. Rev. Lett.* 123, 123601 (2019).
- 43. E. Braaten, H.-W. Hammer, G. P. Lepage, Lindblad equation for the inelastic loss of ultracold atoms. *Phys. Rev. A* **95**, 012708 (2017).
- S. Dürr, J. J. García-Ripoll, N. Syassen, D. M. Bauer, M. Lettner, J. I. Cirac, G. Rempe, Lieb-Liniger model of a dissipation-induced Tonks-Girardeau gas. *Phys. Rev. A* 79, 023614 (2009).
- J. J. García-Ripoll, S. Dürr, N. Syassen, D. M. Bauer, M. Lettner, G. Rempe, J. I. Cirac, Dissipation-induced hard-core boson gas in an optical lattice. *New J. Phys.* 11, 013053 (2009).

Acknowledgments: We thank J. Ye and A. M. Rey for helpful discussions. Funding: Q.Z. and C.L. are supported by NSF PHY 1806796. M.H. is supported by HKRGC through HKUST3/CRF/13G.

SCIENCE ADVANCES | RESEARCH ARTICLE

M.H. and H.-Q.L. acknowledge the financial support from NSAF U1930402 and computational resources from the Beijing Computational Science Research Center. **Author contributions:** Q.Z. conceived the idea. M.H., C.L., H.-Q.L., and Q.Z. contributed to all aspects of this work. Q.Z. and H.L. supervised the project. **Competing interests:** The authors declare that they have no competing interests. **Data and materials availability:** All data needed to evaluate the conclusions in the paper are present in the paper and/or the Supplementary Materials. Additional data related to this paper may be requested from the authors.

Submitted 24 June 2020 Accepted 3 November 2020 Published 18 December 2020 10.1126/sciadv.abd4699

Citation: M. He, C. Lv, H.-Q. Lin, Q. Zhou, Universal relations for ultracold reactive molecules. *Sci. Adv.* **6**, eabd 4699 (2020).

Downloaded from https://www.science.org on December 30, 2021

Science Advances

Universal relations for ultracold reactive molecules

Mingyuan HeChenwei LvHai-Qing LinQi Zhou

Sci. Adv., 6 (51), eabd4699. • DOI: 10.1126/sciadv.abd4699

View the article online

https://www.science.org/doi/10.1126/sciadv.abd4699

Permissions

https://www.science.org/help/reprints-and-permissions